Electrochemistry

DOI: 10.1002/anie.201307137

Ionic-Liquid–Nanoparticle Hybrid Electrolytes: Applications in Lithium Metal Batteries**

*Yingying Lu, Kevin Korf, Yu Kambe, Zhengyuan Tu, and Lynden A. Archer**

Abstract: *Development of rechargeable lithium metal battery (LMB) remains a challenge because of uneven lithium deposition during repeated cycles of charge and discharge. Ionic liquids have received intensive scientific interest as electrolytes because of their exceptional thermal and electrochemical stabilities. Ionic liquid and ionic-liquid–nanoparticle hybrid electrolytes based on 1-methy-3-propylimidazolium (IM) and 1-methy-3-propylpiperidinium (PP) have been synthesized and their ionic conductivity, electrochemical stability, mechanical properties, and ability to promote stable Li electrodeposition investigated. PP-based electrolytes were found to be more conductive and substantially more efficient in suppressing dendrite formation on cycled lithium anodes; as little as 11 wt% PP-IL in a PC-LiTFSI host produces more than a ten-fold increase in cell lifetime. Both PP- and IM-based nanoparticle hybrid electrolytes provide up to 10000-fold improvements in cell lifetime than anticipated based on their mechanical modulus alone. Galvanostatic cycling measurements in $Li/Li_4Ti_5O_{12}$ half cells using IL–nanoparticle hybrid electrolytes reveal more than 500 cycles of trouble-free operation and enhanced rate capability.*

Secondary batteries capable of reliably storing and delivering large amounts of electrical energy are a key component in many contemporary and emerging technologies, such as smart phones, electric vehicles, autonomous aircraft, and advanced robotics.[1–4] Cells with higher operating voltages, improved thermal and cycling stabilities, higher energy densities, enhanced safety, and which offer greater portability are a priority.[5,6] Batteries based on lithium metal anodes are understood to be among the most promising for achieving high specific capacities and high cell voltages.[4,7] Development of a practical rechargeable lithium metal battery (LMB) remains a challenge because of uneven lithium deposition and dendrite formation during repeated cycles of charge and discharge. This results in cell failure modes ranging from accumulation of electrically disconnected regions of the anode or "dead lithium" to internal short-circuits, which limit cell lifetime and may pose serious hazards if a flammable electrolyte is employed. Lithium-ion batteries (LIBs) are designed to eliminate the most serious of these problems by hosting the lithium in a graphitic carbon substrate, but this configuration is not entirely immune from uneven lithium plating and dendrite formation. Specifically, the small potential difference separating lithium intercalation into versus lithium plating onto graphite, means that a too quickly charged or overcharged LIB may fail by similar mechanisms as a LMB.

Researchers have reported many approaches to suppress dendrites or to delay short-circuiting in LMBs. Efforts to-date have focused on all essential components of a battery. Electrodes based on Na-Li[8] alloys or based on pure Li with increased surface area[9,10] have been reported to increase cell lifetimes. Doping the electrode/electrolyte interface (SEI) using electrolyte additives, including ionic liquids[1,11–13] and vinyl silanes[14–15] provide an effective means for smoothening electrodeposition of lithium. Structuring the electrolyte to reduce the anion mobility (e.g. using single ion conductors)[16–18] or to increase the overall mechanical modulus[19–22] have been argued to stabilize Li deposition.[23,24] The general utility of this last approach is challenged by data from sodium batteries, which show that even when a liquid metal anode and hard solid ceramic electrolyte are employed, dendrites form and proliferate through cracks in the ceramic.[25] It is also confounded by the observation that hard metallic magnesium anodes do not form dendritic electrodeposits in a liquid electrolyte.[26] Of the various options, ionic liquids offer multiple synergetic properties that make them attractive electrolytes for extending lifetime and safety of LMBs. Their inherently low vapor pressure, non-flammability, good electrochemical stability in the presence of metallic lithium make ILs excellent choices in fail-safe LMBs. Additionally, ILs based on pyrrolidinium, imidizolium, and piperidinium cations and bis(trifluoro methanesulphonyl)imide (TFSI) counterions have been shown to lead to better electrodeposited lithium morphologies.[24,27–29] Although this effect is not yet understood, continuum theory indicates that immobilization of as little as 10% of the anion by a bulky cation in an electrolyte can reduce ion concentration gradients during polarization, and thereby promote dendrite-free electrodeposition of Li.[18,30]

Inspired by ideas from such theories, we have developed SiO_2-nanoparticle-tethered 1-methy-3-propylimidazolium TFSI (SiO_2-IM-TFSI) and 1-methy-3-propylpiperidinium

[*] Y. Lu, Prof. L. A. Archer
School of Chemical and Biomolecular Engineering
Cornell University, Ithaca, NY 14853 (USA)
E-mail: laa25@cornell.edu
K. Korf, Y. Kambe, Z. Tu
Department of Materials Science and Engineering
Cornell University, Ithaca NY, 14853 (USA)

[**] This material is based on work supported as part of the Energy Materials Center at Cornell, an Energy Frontier Research Center funded by the U.S. Department of Energy, Office of Science, Office of Basic Energy Sciences under award number DESC0001086. Electron microscopy facilities at the Cornell Center for Materials Research (CCMR), an NSF supported MRSEC through grant number DMR-1120296, were also used for the study.

Supporting information for this article is available on the WWW under http://dx.doi.org/10.1002/anie.201307137.

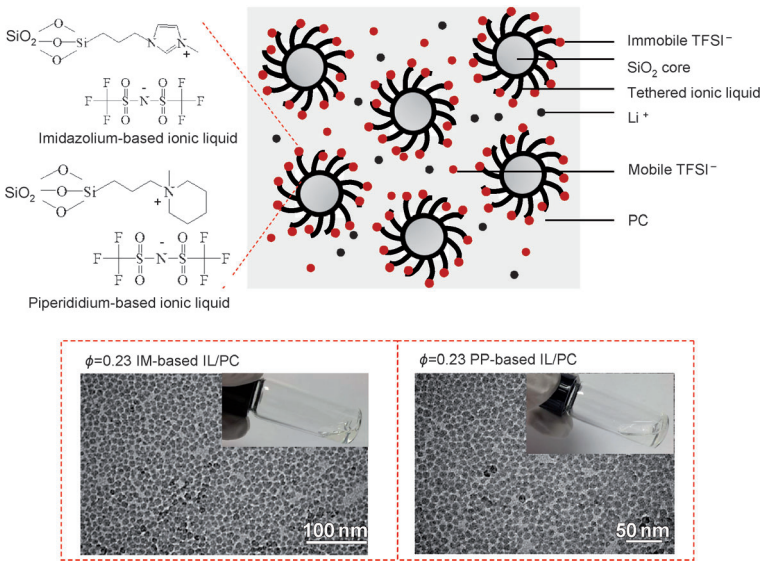

Figure 1. Schematic representation of the SiO_2-IL-TFSI/PC in 1 M LiTFSI hybrid electrolyte system used in the study. TEM images of the electrolytes with $\phi = 0.23$: SiO_2-IM-TFSI (bottom left) and SiO_2-PP-TFSI (bottom right), respectively. The insets display photographs of the two hybrid electrolyte materials showing their fluid-like and homogenous liquid features.

TFSI (SiO_2-PP-TFSI) and created LMB electrolytes (Figure 1) by blending with a propylene carbonate (PC) 1M LiTFSI. The tethered IL component provides a source of nearly immobile, un-dissociated counterions throughout the interelectrode space, potentially allowing for rapid replenishment of counterions upon cell polarization.[30] SiO_2-IL-TFSI nanoparticles were synthesized using previous reported methods.[31,32] PC is chosen as the electrolyte base because it has good miscibility with ILs and is thermally stable up to 242 °C, that is, well above the melting point of lithium metal. Figure 2a reports the DC conductivity for SiO_2-IM-TFSI/PC as a function of the volume fraction ϕ of SiO_2. The corresponding results for the IM-TFSI/PC, SiO_2-PP-TFSI/PC, and PP-TFSI/PC are provided in Figure 2b–d. It is apparent that electrolytes with intermediate ϕ exhibit conductivities above 10^{-3} S cm^{-1} at room temperature. The results for the PP-based electrolytes are particularly remarkable, as conductivities approaching 1 mS cm^{-1} are observed even at ϕ of about 0.48.

The suitability of the SiO_2-IL-TFSI/PC electrolytes for LMBs was investigated in Li/$Li_4Ti_5O_{12}$ half cells. $Li_4Ti_5O_{12}$ (LTO) is a good choice because of its stable cycling at low and high rates with close to the theoretical capacities (175 mAh g^{-1}) and negligible round-trip IR losses.[33,34] Figure 3a–c shows that irrespective of the IL chemistry, these cells are stable for more than 500 cycles. Figure 3d further shows that irrespective of the IL, SiO_2-IL-TFSI/PC electrolytes exhibit weaker rate dependences. Considering the moderately lower conductivity of the materials, this is a surprising result. We believe it stems from the greater interface stability of the SiO_2-IL-TFSI/PC electrolytes.

To investigate the influence of the IL–hybrid electrolytes on electrodeposition of Li, a cyclic lithium plate-strip procedure comprised of three hours of charge followed by three hours of discharge was used to evaluate the cells over hundreds of cycles. The three-hour period mimics the charge/discharge profiles of typical cells and allows enough lithium to be transported during each cycle to create dendrites that are large enough to short-circuit the cell. Figure 4a,b shows a typical voltage response obtained with pure PC and hybrid SiO_2-IM-TFSI/PC. The pure PC electrolyte requires an induction period of several cycles to achieve a steady-state voltage, the hybrid electrolyte reaches steady state quickly. After a small number of cycles, the peak-to-peak voltage of the PC electrolyte begins to fall and the cell quickly fails. In contrast, the voltage profile for the SiO_2-IM-TFSI/PC electrolyte is stable for a much larger number of cycles. To obtain a quantitative measure of the relative performance of the various electrolytes, we arbitrarily defined the end-of-life of the cells as the time T_d at which the peak-to-peak voltage amplitude drops by at least 20% (see Figure S4 in the Supporting Information). The charge passed during the cell lifetime C_d is the product of T_d and the current density J. Figure 4c reports T_d versus J and it is apparent that IM-TFSI alone has a large effect on T_d, and SiO_2-IM-TFSI extend lifetime by an order of magnitude or more, relative to pure PC. Figure 4d reports $1/C_d$ as a function of the shear modulus G^* of the SiO_2-IM-TFSI/PC electrolytes. It is apparent that there is a rough inverse correlation between $1/C_d$ and G^*, but the profiles extrapolate to a $1/C_d \approx 0$ (i.e. $T_d \rightarrow \infty$), at G^* between 10^3 and 10^5 Pa, which is at least four orders of magnitude lower than predicted for mechanical reinforcement alone.[23]

A more aggressive polarization procedure has been employed previously for characterizing lith-

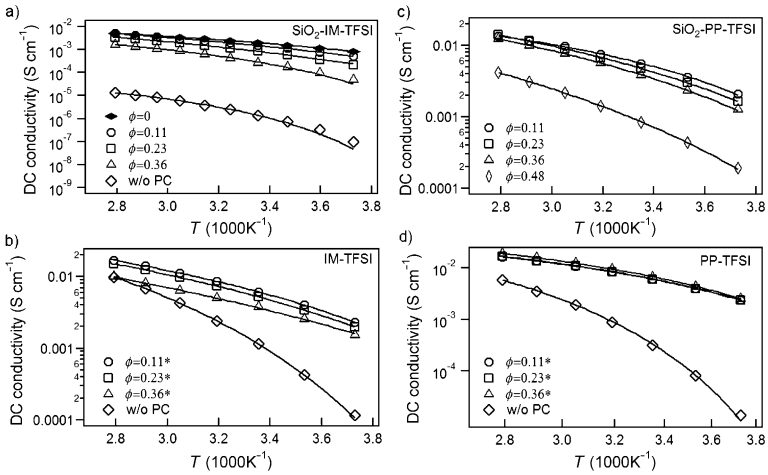

Figure 2. Direct current conductivities as a function of temperature for a) SiO_2-IM-TFSI, b) IM-TFSI, c) SiO_2-PP-TFSI, and d) PP-TFSI with different amounts of PC in 1 M LiTFSI. ϕ is the volume fraction of silica nanoparticles in the electrolytes. The solid lines are best fits using the VFT expression for the temperature-dependent DC conductivity. The asterisked values are results for IL-TFSI/PC with an equivalent IL concentration as the SiO_2-IL-TFSI/PC systems.

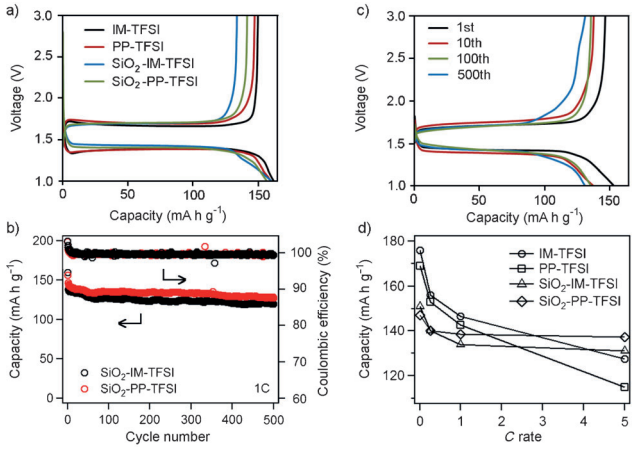

Figure 3. Charge–discharge characteristics of Li/LTO full batteries with IM-TFSI, PP-TFSI, SiO_2-IM-TFSI, SiO_2-PP-TFSI electrolytes at intermediate chain loading, $\phi = 0.23$. a) Initial charge–discharge curves at a current density of 0.315 mA cm^{-2} (1C). b) Discharge capacity versus cycle number of the two hybrid electrolyte systems and c) initial, 10th, 100th, 500th charge–discharge curves of SiO_2-PP-TFSI electrolytes in lithium metal/LTO batteries at room temperature. d) Capacity versus charge (*C*) rate for the four electrolytes studied.

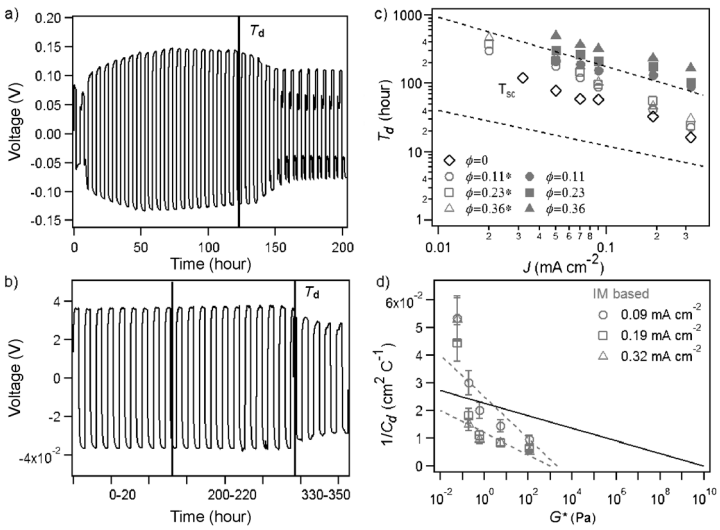

Figure 4. a) Voltage versus time for a symmetric lithium cell containing pure PC in 1 M LiTFSI cycled using the plate-strip scheme described in the text at a fixed current density *J* of 0.03 mA cm^{-2}. b) Same as (a) except the electrolyte is SiO_2-IM-TFSI/PC 1 M LiTFSI hybrid electrolyte and $J = 0.09$ mA cm^{-2}. c) Short-circuit time (T_d) determined as the time required for the peak-to-peak voltage to decrease by 20% relative to its steady-state value, as a function of current density. The open and filled red markers are IM-TFSI and SiO_2-IM-TFSI, respectively, and the dashed lines in the plot are results from galvanostatic polarization measurements described in the next section for pure PC and the IL-based electrolytes. d) Reciprocal of charge passed before short circuit ($1/C_d$) as a function of complex modulus *G** at various current densities. The continuous solid lines are extrapolated from the best fit profile reported in Ref. [21].

ium electrodeposition and LMB cell failure in symmetric lithium cells.[17] In this approach the cell is polarized at fixed *J* and the voltage measured as a function of time. Typical

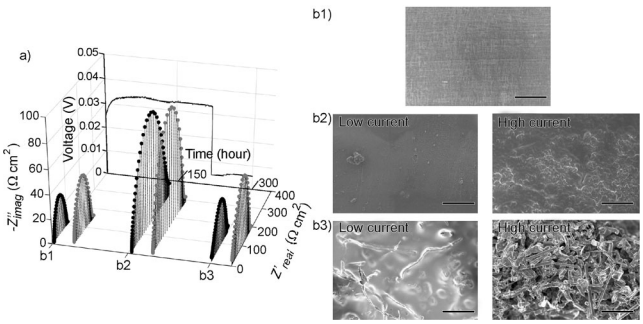

Figure 5. Potential profile at fixed current density, impedance spectroscopy, and SEM images for $\phi = 0.23$: IM-TFSI (black) and SiO_2-IM-TFSI (red) at three stages, a) before polarization, b) during steady state, and c) after cell short-circuit. The right and left sets of SEM images are the results from low-current density (e.g. 0.02 mA cm^{-1}) and high-current density (e.g. 0.1 mA cm^{-1}) charges, respectively. The scale bar for all SEM images is 100 μm.

voltage profiles for electrolytes with $\phi = 0.23$ are shown in Figure 5a and Figure S5. The time at which the sudden voltage drop occurs provides an estimate for the time-to-failure by short-circuits, T_{SC}. Impedance spectra at different stages of polarization (Figure 5a) and post-mortem SEM analysis of the lithium electrode from cells interrupted at these same stages (Figure 5b1–3) indicate that the sudden voltage drop coincides with appearance of micron-scale, fibrous structures on the lithium metal surface. The width of the impedance spectra rises substantially after the polarization begins and drops abruptly at cell failure. It means that even before nonuniform electrodeposits are apparent by SEM observation, they are probably already present as evidenced by the greater difficulty in depositing Li. Figure 6 provides additional detail about the effectiveness of PP- and IM-based electrolytes for extending LMB lifetime. In contrast to the plate-strip experiments, for which T_d for the SiO_2-IL-TFSI/PC electrolytes were consistently greater than for the IL-TFSI/PC, the results in Figure 6 indicate that an IL-TFSI/PC electrolyte with comparable IL content provides a measurably larger increase in cell lifetime. We suspect that this arises from the higher room-temperature conductivity of the IL-TFSI/PC electrolytes. It is also apparent that whereas T_{SC} for cells based on IM electrolytes depend on the IL concentration, T_{SC} is nearly independent of IL composition for PP-based electrolytes. This finding suggests that PP is more efficient in promoting uniform Li electrodeposition, perhaps due to the greater ease of dissociating the PP-TFSI ionic bond.

In summary, ionic-liquid and ionic-liquid–nanoparticle hybrid electrolytes based on 1-methy-3-propylimidazolium (IM) and 1-methy-3-propylpiperidinium (PP) have been synthesized and their ionic conductivity, electrochemical stability, mechanical properties, and ability to promote stable Li electrodeposition investigated. We find that PP-based electrolytes are more conductive and substantially more efficient in suppressing cell short circuiting. As little as 11 w% of SiO_2-PP-TFSI in a PC-LiTFSI host produces more than a ten-fold increase in cell lifetime. IM-based electrolytes produce similar levels of Li dendrite suppression, but require

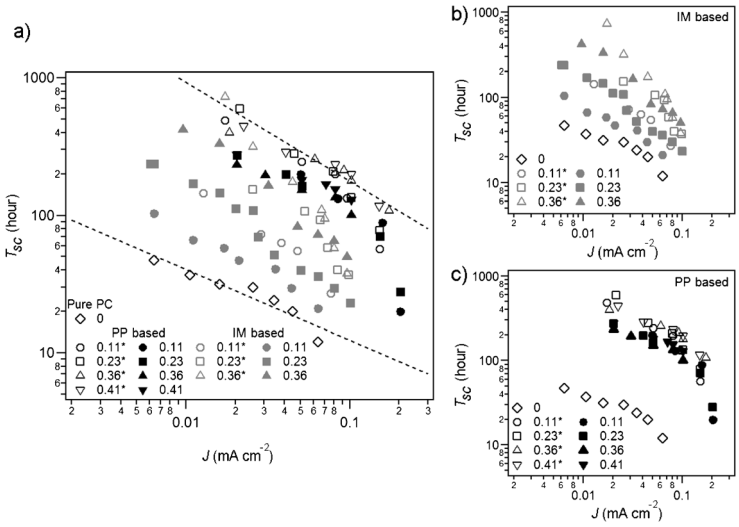

Figure 6. a) Short-circuit time T_{SC} as a function of current density J from galvanostatic polarization measurements for symmetric lithium cells. Filled red and black markers represent imidazolium and piperidinium-based IL-nanoparticle hybrid electrolytes, and open markers represent the corresponding free IL-based electrolytes. The dashed lines are power-law fits to the data. Figure 6b) and c) are extracted from 6a to compare performance of particle-tethered and free imidazolium and piperidinium-based IL electrolytes.

higher IL and/or nanoparticle concentrations. Both materials provide up to 10000-fold and more improvement in cell lifetime than anticipated based on their mechanical modulus alone. Galvanostatic cycling measurements in $Li/Li_4Ti_5O_{12}$ half cells using IL–nanoparticle hybrid electrolytes reveal more than 500 cycles of trouble-free operation and enhanced rate capability.

Experimental Section

Methods: SiO_2-IL-TFSI/PC in 1M lithium bis(trifluoromethanesulfonyl)imide (LiTFSI) was prepared using our previously reported method.[31,32] The grafting densities of PP-TFSI and IM-TFSI on the silica nanoparticles estimated using thermal gravimetric analysis are around 1.2 and 0.9 chains nm^{-2}, respectively. As the synthesis occurs in water, it is necessary to implement a rigorous, multi-step drying protocol to avoid contamination of the electrolytes by residual moisture. To prepare the anhydrous solution, LiTFSI was dried at 110°C for four hours and then at 170°C for three days under vacuum. Propylene carbonate was kept on 3 Å sieves for at least one week and 1M LiTFSI in IL-TFSI/PC was then prepared in a glovebox. For SiO_2-IL-TFSI/PC electrolyte system, SiO_2-IL-TFSI the solution was first dried at 50°C for 5 days, then under vacuum at 45°C for one day, and finally freeze-dried for one day. The broad IR band centered at around 3500 cm^{-1} is well-known for its sensitivity to water. Figure S6 is the FTIR spectrum for a representative SiO_2-PP-TFSI/PC in 1M LiTFSI electrolyte following the drying process. A Seiko Instrument TG-DTA6200 was used for thermal analysis. Symmetric lithium metal coin cells were used for dielectric and impedance spectroscopy, galvanostatic polarization, and cycling measurements. A Novocontrol N40 broadband spectrometer was used for ionic conductivity measurements. A Neware CT-3008 battery tester was used for galvanostatic polarization and cycling studies. Impedance spectra were measured as a function of frequency at room temperature using Solartron frequency response analyzer (model 1252). Cells were disassembled and the lithium metal electrodes were harvested and analyzed by scanning electron microscopy (SEM, LEO1550-FESEM). LTO spinel nanopowder with particle size >100 nm, Super P carbon black, and PVDF (polyvinylidene difluoride), were mixed in a 80:10:10 weight ratio in *N*-methylpyrrolidone (NMP). The copper foil was coated with the viscous slurry using a film casting doctor blade (MTI Corporation) and dried in a vacuum oven overnight. The electrodes were calendared and punched out of the film with a 0.5 inch diameter.

Received: August 14, 2013
Revised: October 15, 2013
Published online: November 26, 2013

Keywords: electrolytes · ionic liquids · lithium dendrites · lithium metal battery · nanoparticles

[1] R. Bhattacharyya, B. Key, H. Chen, A. S. Best, A. F. Hollenkamp, C. P. Grey, *Nat. Mater.* **2012**, *11*, 504–510.
[2] M. Tran, D. Banister, J. D. K. Bishop, M. D. McCulloch, *Nat. Clim. Change* **2012**, *2*, 328–333.
[3] M. Armand, J.-M. Tarascon, *Nature* **2008**, *451*, 652–657.
[4] J.-M. Tarascon, M. Armand, *Nature* **2001**, *414*, 359–367.
[5] A. S. Aricò, P. Bruce, B. Scrosati, J.-M. Tarascon, W. V. Schalkwijk, *Nat. Mater.* **2005**, *4*, 366–377.
[6] P. G. Bruce, S. A. Freunberger, L. J. Hardwick, J.-M. Tarascon, *Nat. Mater.* **2012**, *11*, 19–29.
[7] K. Xu, *Chem. Rev.* **2004**, *104*, 4303–4417.
[8] J. K. Stark, Y. Ding, P. A. Kohl, *J. Electrochem. Soc.* **2011**, *158*, A1100–A1105.
[9] W.-S. Kim, W.-Y. Yoon, *Electrochim. Acta* **2004**, *50*, 541–545.
[10] A. Zhamu, G. Chen, C. Liu, D. Neff, Q. Fang, Z. Yu, W. Xiong, Y. Wang, X. Wang, B. Z. Jang, *Energy Environ. Sci.* **2012**, *5*, 5701–5707.
[11] N. Byrne, P. C. Howlett, D. R. MarFarlane, M. Forsyth, *Adv. Mater.* **2005**, *17*, 2497–2501.
[12] H. Sano, H. Sakaebe, H. Matsumoto, *J. Power Sources* **2011**, *196*, 6663–6669.
[13] S. Liu, N. Imanishi, T. Zhang, A. Hirano, Y. Takeda, O. Yamomoto, J. Yang, *J. Electrochem. Soc.* **2010**, *157*, A1092–A1098.
[14] S.-K. Jeong, H.-Y. Seo, D.-H. Kim, H.-K. Han, J.-G. Kim, Y. B. Lee, Y. Iriyama, T. Abe, Z. Ogumi, *Electrochem. Commun.* **2008**, *10*, 635–638.
[15] Y. M. Lee, J. E. Seo, Y.-G. Lee, S. H. Lee, K. Y. Cho, J.-K. Park, *Electrochem. Solid-State Lett.* **2007**, *10*, A216–A219.
[16] C. Brissot, M. Rosso, J.-N. Chazalviel, S. Lascaud, *J. Power Sources* **1999**, *81–82*, 925–929.
[17] M. Rosso, T. Gobron, C. Brissot, J.-N. Chazalviel, S. Lascaud, *J. Power Sources* **2001**, *97–98*, 804–806.
[18] J.-N. Chazalviel, *Phys. Rev. A* **1990**, *42*, 7355–7367.
[19] J. L. Schaefer, D. L. Yanga, L. A. Archer, *Chem. Mater.* **2013**, *25*, 834–839.
[20] G. M. Stone, S. A. Mullin, A. A. Teran, D. T. Hallinan Jr. , A. N. Minor, A, Hexemer, N. P. Balsara, *J. Electrochem. Soc.* **2012**, *159*, A222–A227.
[21] C. Monroe, J. Newman, *J. Electrochem. Soc.* **2005**, *152*, A396–A404.
[22] Z. Tu, Y. Kambe, Y. Lu, L. A. Archer, *Adv. Energy Mater.* **2013**, DOI: 10.1002/aenm.201300654.
[23] C. Monroe, J. Newman, *J. Electrochem. Soc.* **2003**, *150*, A1377–A1384.
[24] S. S. Moganty, S. Srivastava, Y. Lu, J. L. Schaefer, S. A. Rizvi, L. A. Archer, *Chem. Mater.* **2012**, *24*, 1386–1392.

[25] R. O. Ansell, *J. Mater. Sci.* **1986**, *21*, 365 – 379.
[26] D. Aurbach, Z. Lu, A. Schechter, Y. Gofer, H. Gizbar, R. Turgeman, Y. Cohen, M. Moshkovich, E. Levi, *Nature* **2000**, *407*, 724 – 727.
[27] M. Armand, F. Endres, D. R. MacFarlane, H. Ohno, B. Scrosati, *Nat. Mater.* **2009**, *8*, 621 – 629.
[28] N. Jayaprakash, J. Shen, S. S. Moganty, A. Corona, L. A. Archer, *Angew. Chem.* **2011**, *123*, 6026 – 6030; *Angew. Chem. Int. Ed.* **2011**, *50*, 5904 – 5908.
[29] S. S. Moganty, N. Jayaprakash, J. L. Nugent, J. Shen, L. A. Archer, *Angew. Chem.* **2010**, *122*, 9344 – 9347; *Angew. Chem. Int. Ed.* **2010**, *49*, 9158 – 9161.
[30] M. Tikekar, D. L. Koch, L. A. Archer, "Stability analysis of electrodeposition in a structured electrolyte comprised of fixed anions," submitted.
[31] Y. Lu, S. S. Moganty, J. L. Schaefer, L. A. Archer, *J. Mater. Chem.* **2012**, *22*, 4066 – 4072.
[32] Y. Lu, S. K. Das, S. S. Moganty, L. A. Archer, *Adv. Mater.* **2012**, *24*, 4430 – 4435.
[33] T. Brousse, P. Fragnaud, R. Marchand, D. M. Schleich, O. Bohnke, K. West, *J. Power Sources* **1997**, *68*, 412 – 415.
[34] K. Nakahara, R. Nakajima, T. Matsushima, H. Majima, *J. Power Sources* **2003**, *117*, 131 – 136.

